

EXAMINATION OF THE MECHANISM OF N-ACETYL-1-D-MYO-INOSITYL-2-AMINO-2-DEOXY- α -D-GLUCOPYRANOSIDE DEACETYLASE (MSHB)
REVEALS AN UNEXPECTED ROLE FOR A DYNAMIC TYROSINE

Xinyi Huang and Marcy Hernick* \dagger

Department of Biochemistry, Virginia Tech, Blacksburg, VA 24061

SUPPLEMENTAL DATA

Contents:

Table S1. Effect of solvent viscosity on WT MshB

Table S2. Effect of solvent viscosity on MshB mutants (k_{cat})

Table S3. Effect of solvent viscosity on MshB mutants (k_{cat}/K_M)

Figure S1. Effect of solvent viscosity on activity (k_{cat}) of H144A

Figure S2. Effect of NaCl on MshB activity

Figure S3. Michealis-Menten plot for steady-state turnover by MshB mutants

Figure S4. Effect of solvent viscosity on MshB activity (k_{cat}/K_M)

Figure S5. NaF inhibition of MshB

Figure S6. Solvent isotope effect of MshB under V conditions

Figure S7. Activation of apo-D146A MshB with titrating amounts of Zn^{2+}

Figure S8. Hydrophobicity and Surface Area Correlation Plots for position 142

Table S1. Effect of solvent viscosity on WT MshB

MshB variant ^a	Viscogen	Y-axis	X-axis	Slope	R ²
WT	Glycerol	$^{\circ}k_{\text{cat}}/k_{\text{cat}}$	η_{rel}	0.74 ± 0.13	0.945
	Sucrose			0.62 ± 0.11	0.911
	Ficoll			0.03 ± 0.006	0.956
WT	Glycerol	$(^{\circ}k_{\text{cat}}/K_{\text{M}})/(k_{\text{cat}}/K_{\text{M}})$	η_{rel}	1.72 ± 0.12	0.990
	Sucrose			1.70 ± 0.28	0.924
	Ficoll			-0.086 ± 0.02	0.958
WT	Glycerol	$\log (^{\circ}k_{\text{cat}}/k_{\text{cat}})$	$\log (\eta_{\text{rel}})$	0.72 ± 0.09	0.889
	Sucrose			0.81 ± 0.06	0.878
	Ficoll			0.05 ± 0.01	0.810
WT	Glycerol	$\log (^{\circ}k_{\text{cat}}/k_{\text{cat}})$	η_{rel}^2	0.044 ± 0.005	0.923
	Sucrose			0.095 ± 0.01	0.571
	Ficoll			0.005 ± 0.0003	0.983
WT	Glycerol	$\log (^{\circ}k_{\text{cat}}/K_{\text{M}})/(k_{\text{cat}}/K_{\text{M}})$	$\log (\eta_{\text{rel}})$	1.45 ± 0.09	0.975
	Sucrose			1.57 ± 0.2	0.852
	Ficoll			-0.19 ± 0.05	0.890
WT	Glycerol	$\log (^{\circ}k_{\text{cat}}/K_{\text{M}})/(k_{\text{cat}}/K_{\text{M}})$	η_{rel}^2	0.044 ± 0.15	0.778
	Sucrose			0.045 ± 0.13	0.822

^a apo-MshB was incubated with stoichiometric Zn²⁺ for 30 min prior to activity measurement with a sub-saturating concentration (5 mM) or saturating concentration (100 mM) of GlcNAc as described in “Materials and Methods”. A linear equation was fit to the resulting data. Select graphical representations of data are shown in Figures 2 and S4.

Table S2. Effect of solvent viscosity on MshB mutants (k_{cat})

MshB Variant ^a	Viscogen	Y-axis	X-axis	Slope	R ²
D15A	Glycerol	$^{\circ}k_{cat}/k_{cat}$	η_{rel}	1.62 ± 0.18	0.975
	Sucrose			1.80 ± 0.19	0.967
Y142F	Sucrose			0.01 ± 0.02	0.075
H144A	Glycerol			0.53 ± 0.04	0.988
	Sucrose			0.14 ± 0.02	0.967
D15A	Glycerol	$\log (^{\circ}k_{cat}/k_{cat})$	$\log (\eta_{rel})$	1.37 ± 0.07	0.973
	Sucrose			1.39 ± 0.06	0.982
Y142F	Sucrose			-0.02 ± 0.02	0.041
H144A	Glycerol			1.09 ± 0.03	0.991
	Glycerol ^b			0.92 ± 0.09	0.927
	Sucrose			0.33 ± 0.03	0.947
D15A	Glycerol	$\log (^{\circ}k_{cat}/k_{cat})$	η_{rel}^2	0.082 ± 0.01	0.920
	Sucrose			0.081 ± 0.005	0.980
Y142F	Sucrose			-0.001 ± 0.001	0.327
H144A	Glycerol			0.065 ± 0.006	0.950
	Sucrose			0.02 ± 0.002	0.972

^a apo-MshB was incubated with stoichiometric Zn²⁺ for 30 min prior to activity measurement with a saturating concentration (100mM) of GlcNAc as described in “Materials and Methods”. Select graphical representations of data are shown in Figures 2, 3, and S4. ^b Substrate = 300 mM GlcNAc

Table S3. Effect of solvent viscosity on MshB mutants (k_{cat}/K_M)

MshB Variant ^a	Viscogen	Y-axis	X-axis	Slope	R ²
Y142F	Sucrose	$(^{\circ}k_{cat}/K_M)/(k_{cat}/K_M)$	η_{rel}	0.31 ± 0.03	0.960
D146A	Glycerol			0.30 ± 0.05	0.976
	Sucrose			0.03 ± 0.02	0.731
Y142F	Sucrose	$\log (^{\circ}k_{cat}/K_M)/(k_{cat}/K_M)$	$\log \eta_{rel}$	0.48 ± 0.03	0.957
D146A	Glycerol			0.40 ± 0.03	0.937
	Sucrose			0.05 ± 0.01	0.551
Y142F	Sucrose	$\log (^{\circ}k_{cat}/K_M)/(k_{cat}/K_M)$	η_{rel}^2	0.04 ± 0.03	0.864
D146A	Glycerol			0.03 ± 0.003	0.957
	Sucrose			0.003 ± 0.001	0.547

^a apo-MshB was incubated with stoichiometric Zn²⁺ for 30 min prior to activity measurement with a sub-saturating concentration of GlcNAc (5 mM, Y142F; 50 mM, D146A) as described in “Materials and Methods”. A linear equation was fit to the resulting data. Select graphical representations of data are shown in Figure S4.

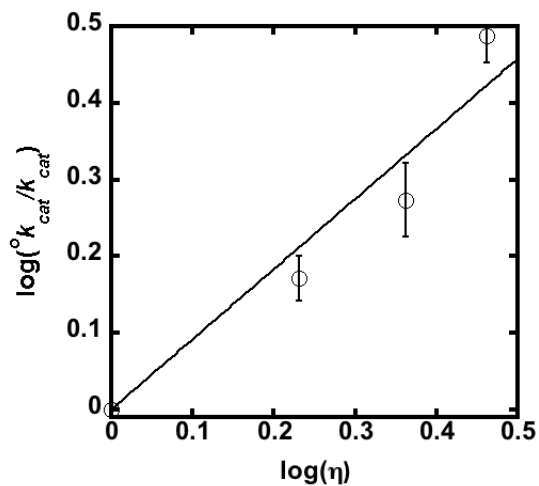


Figure S1. Effect of solvent viscosity activity (k_{cat}) of H144A. The effects of the microviscogen glycerol (0-35% (w/v)) on H144A MshB. Apo-MshB was incubated with stoichiometric Zn^{2+} . After 30 minutes, the enzyme was diluted into assay buffer (50 mM HEPES, 1 mM TECP, 50 mM NaCl pH 7.5) containing substrate and the initial rates for the deacetylation of saturating concentration (300 mM) GlcNAc as described under “Materials and Methods”. The slopes are provided in Supplemental Data Table S1.

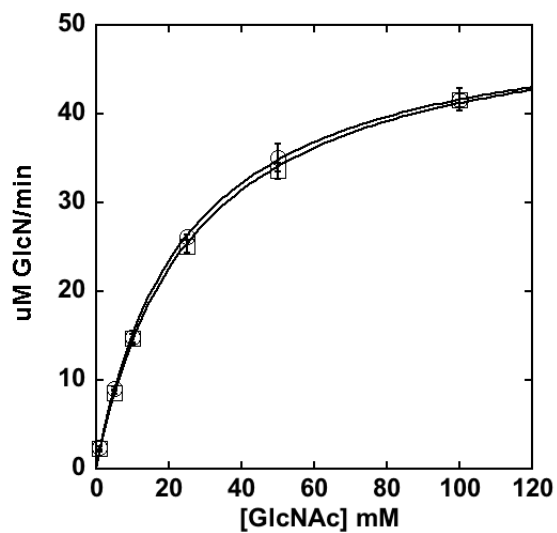


Figure S2: Effect of NaCl on MshB activity. Steady-state turnover of Zn^{2+} -MshB in the presence of (○) 50 mM NaCl or (□) 250 mM NaCl. Apo-MshB was incubated with stoichiometric Zn^{2+} . After 30 minutes, the enzyme was diluted into assay buffer containing substrate and the initial rates for the deacetylation of GlcNAc (0-100 mM) were measured at 30 °C as described in “Materials and Methods”. The steady-state parameters k_{cat} , K_{M} , and $k_{\text{cat}}/K_{\text{M}}$ (Table 1) were obtained by fitting the Michaelis-Menten equation to the initial rates.

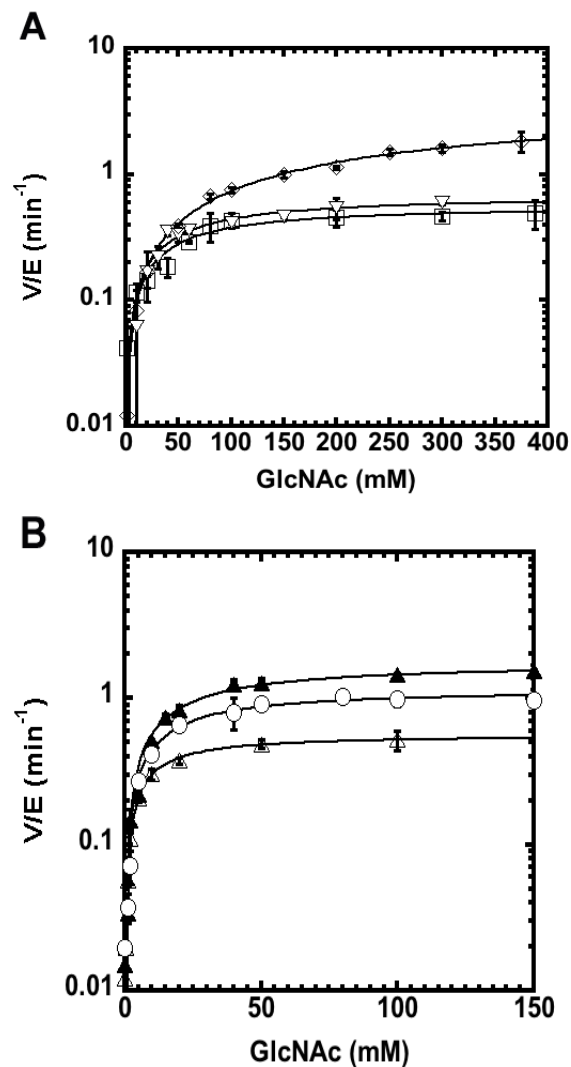


Figure S3: Michealis-Menten plot for steady-state turnover by MshB mutants. GlcNAc (0-375 mM) was pre-equilibrated at 30 °C in assay buffer (50 mM HEPES, 50 mM NaCl, 1 mM TCEP pH 7.5) and the reaction was initiated by the addition of MshB. The resulting activity was measured as described in “Materials and Methods”. The steady-state parameters k_{cat} , K_M , and k_{cat}/K_M were obtained by fitting the Michaelis-Menten equation to the initial rates and are shown in Table 1.

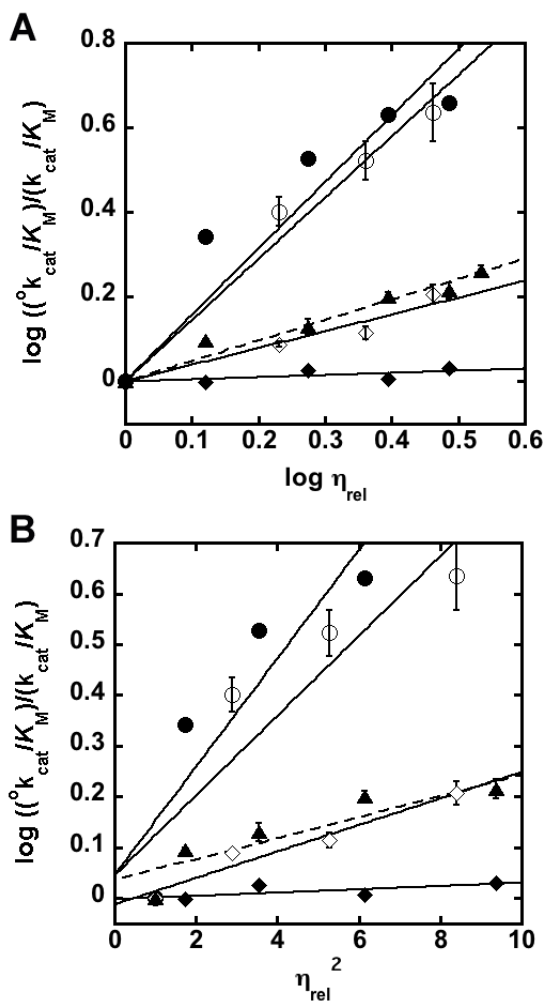


Figure S4: Effect of solvent viscosity on MshB activity (k_{cat}/K_M). The effects of the microviscogens sucrose (0-35% (w/v)) and glycerol (0-35% (w/v)) on WT MshB are depicted as (●) and (○), respectively. The effects of the microviscogens sucrose (0-35% (w/v)) and glycerol (0-35% (w/v)) on D146A MshB are depicted as (◆) and (◇), respectively, while the effect of sucrose (0-35% (w/v)) on Y142F is depicted as (▲). Apo-MshB was incubated with stoichiometric Zn^{2+} . After 30 minutes, the enzyme was diluted into assay buffer (50 mM HEPES, 1 mM TECP, 50 mM NaCl pH 7.5) containing substrate and the initial rates for the deacetylation of sub-saturating concentration (WT, 5 mM; D146A, 50 mM) GlcNAc as described under “Materials and Methods”.

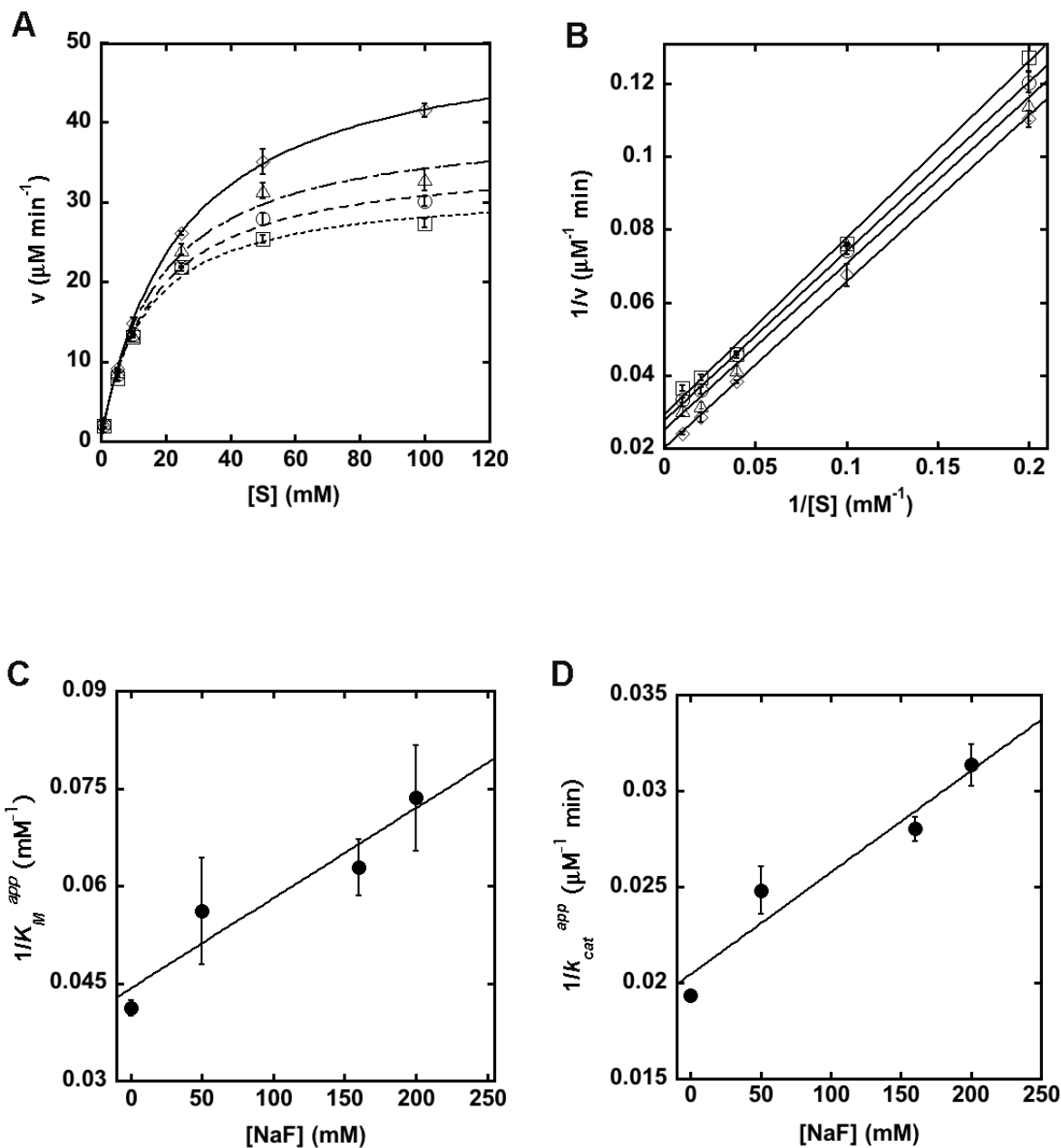


Figure S5: NaF inhibition of MshB activity. (A) Michaelis-Menten plot and (B) double-reciprocal plot of Zn^{2+} -MshB activity at various fluoride concentrations. Fluoride concentrations were 0 (\diamond), 50 (\triangle), 160 (\circ), and 200 (\square) mM. The parallel lines in panel (B) are indicative of uncompetitive inhibition. Replots showing the linear relationships between (C) $1/K_M^{\text{app}}$ and (D) $1/k_{\text{cat}}^{\text{app}}$ and fluoride concentration. Assays were performed at 30°C (50 mM HEPES, 1 mM TECP, 50mM NaCl pH 7.5) with various concentrations of GlcNAc as described under “Materials and Methods”. The K_I values for fluoride are estimated to be 0.32 and 0.38 M for $1/K_M^{\text{app}}$ and $1/k_{\text{cat}}^{\text{app}}$, respectively.

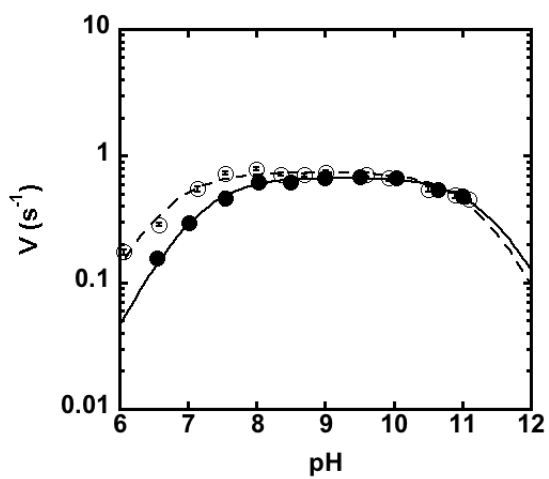


Figure S6: Solvent isotope effect of MshB. The solvent isotope for MshB was measured in H₂O (○) and 95% D₂O (●) at 30°C. Solvent isotope effects were measured under saturating substrate concentrations of GlcNAc (100 mM) as described under “Materials and Methods”. The pK_a values were determined by fitting an equation with two ionizations (Eq. 1) to these data and are 7.1 ± 0.1 and 11.4 ± 0.1, respectively.

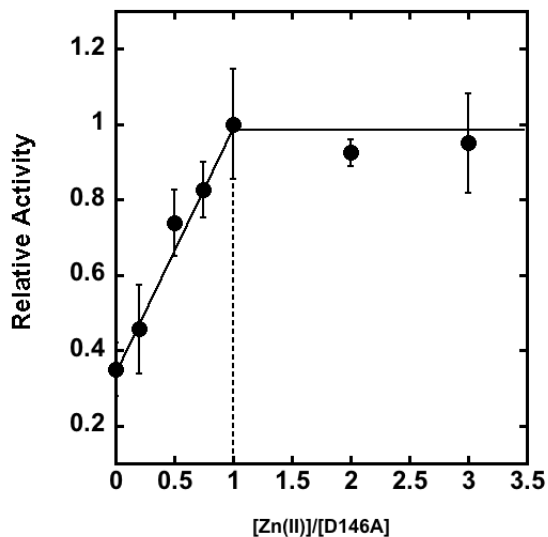


Figure S7: Activation of apo-D146A MshB with Zn^{2+} . Fe^{2+} Deacetylase activity was measured as a function of Me^{2+} /MshB stoichiometry. Apo-MshB was incubated with varying equivalents of Me^{2+} (0-3). After 30 minutes, the enzyme was diluted into assay buffer containing substrate GlcNAc (50 mM) and the resulting deacetylase activity was measured at 30 °C as described in “Materials and Methods”.

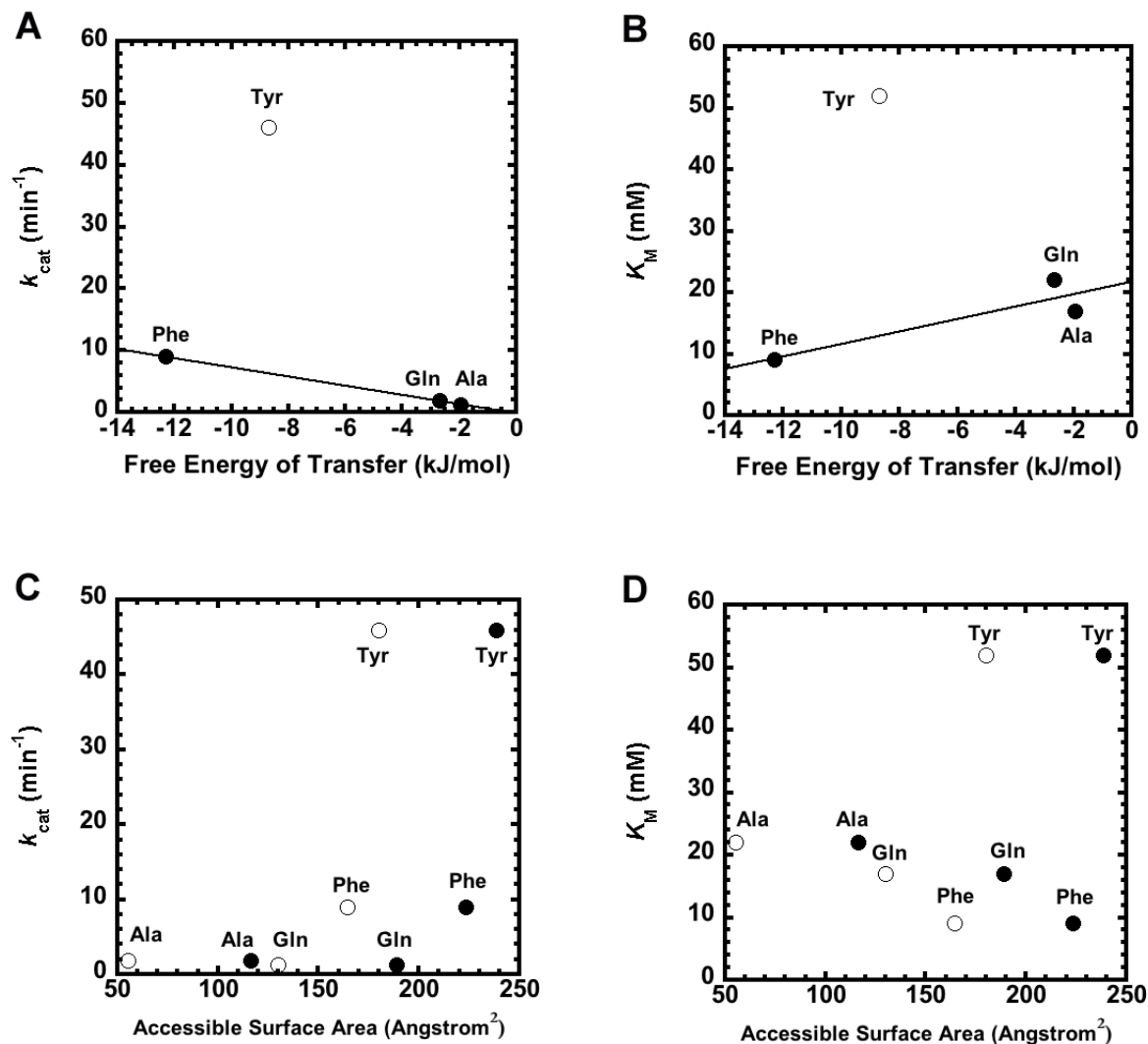


Figure S8: Hydrophobicity and Surface Area Correlation Plots for position 142. (A) Plot of k_{cat} vs. hydrophobicity (Free Energy of Transfer(1)) at position 142. Slope = 0.75 and $R^2 = 0.99995$. (B) Plot of K_M vs. hydrophobicity (Free Energy of Transfer(1)) at position 142. Slope = 1.02 and $R^2 = 0.8081$. (C) Plot of k_{cat} vs. Accessible Surface Area (2) for whole residue (●) or side chain (○). (D) Plot of K_M vs. Accessible Surface Area (2) for whole residue (●) or side chain (○).

1. Chan, H. S. (2002) Amino Acid Side-chain Hydrophobicity. in *Encyclopedia of Life Sciences (eLS)*, John Wiley & Sons, Ltd. pp 1-7
2. Samanta, U., Bahadur, R. P., and Chakrabarti, P. (2002) *Protein Eng.* **15**, 659-667